A Method of Eliminating Interreflection in 3D Reconstruction using Structured Light 3D Camera

Lam Quang Bui[1] and Sukhan Lee[1, 2]
[1]*Colleage of Information and Communication Enginerring, Sungkyunkwan University, Suwon, Korea*
[2]*Department of Interaction Science, Sungkyunkwan University, Seoul, Korea*

Keywords: Interreflection, Structured Light 3D Camera.

Abstract: Interreflection, which is one of main components of the global illumination effect, degrades the performance of structured light 3D camera. In this paper, we present a method of eliminating interreflection in 3D reconstruction using structured light 3D camera without any modification of the structured light pattern. The key idea is to rely on the patterns in final layer of HOC (Hierarchical Orthogonal Coding), where the effect of interreflection is weakest due to small light stripes in the pattern, to eliminate the reflected boundaries as well as fill the missing boundaries in upper layers. Experimental results show that the effect of interreflection in proposed algorithm is significantly reduced in comparison with original decoding method of HOC. The proposed method can be readily incorporated into existing structured light 3D cameras without any extra pattern or hardware.

1 INTRODUCTION

Interreflection is a process where the light from a light source is reflected from an object and hits other objects in the surrounding area, as shown in Figure 1. In 3D computer graphics, interreflection is an important component of global illumination. In 3D reconstruction using structured light based 3D camera, interreflection causes the error in 3D reconstruction of the surface where both interreflection and direct light appear, thus removing or identifying the interreflection has drawn much attentions from computer vision community.

Forsyth et al. (Forsyth, 1989; 1990) are the pioneers in studying the effect of interreflection and its impacts on object shape reconstruction. The analytic solution was presented and tested on concave objects with varying albedo value. They also demonstrated that the effect of interreflection depends on the albedo of object surface, the same object with smaller albedo value exhibits less interreflections. This effect is caused by the non-linearity of the m-bounced light with respect to the surface albedo. However, the authors did not exploit more on non-linearity property of m-bounced light to remove the interreflection in shape recovery. Instead, they claimed that the object shape can be reconstructed by constructing a dictionary of the most common interrefection can occur, and using this dictionary to estimate object shape.

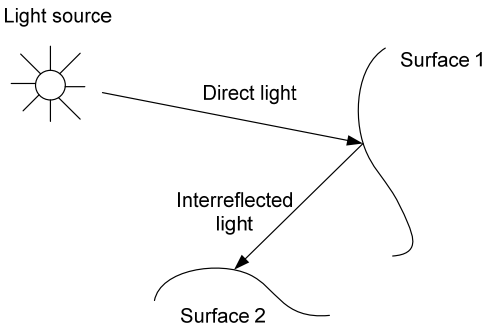

Figure 1: The direct light from light source hits the first surface, then the reflected light hits the second surface, which is called interreflection.

Drew et al. (Funt, 1993; Funt, 1991; Ho, 1990) separated the interreflection from direct lighting by using the color bleeding effect. However, they had to make several assumptions depending on the scene in order to apply their algorithm.

Nayar et al. (Nayar, 1991) solved the problem of shape from interreflection by iteratively refining the shape and reflectance. The algorithm starts to iterate with the initial estimation of shape and reflectance in the presence of the interreflection. The

Quang Bui L. and Lee S..
A Method of Eliminating Interreflection in 3D Reconstruction using Structured Light 3D Camera.
DOI: 10.5220/0004744906400647
In *Proceedings of the 9th International Conference on Computer Vision Theory and Applications* (VISAPP-2014), pages 640-647
ISBN: 978-989-758-009-3

interreflection is estimated based on the reconstructed shape and reflectance of the surface, and in next iteration, this estimated interreflection is compensated to compute the shape and reflectance. In their follow-up work (Nayar, 1992), the authors extended the algorithm to deal with colored and multi-colored surfaces. Due to the fact that the reflectance of a color surface point is dependent on the incident light spectrum, the algorithm is applied to the three chanels of color images independently. However, their method can not handle occlusions. The occluded part, which can add the interreflection to the scene, is not considered at the time of estimating the initial guess of the shape and reflectance. A bad initial guess of the object shape and reflectance could lead to the failure of convergence of the algorithm.

Nayar et al. (Nayar, 2006) introduced a method of separating the direct light from global light for complex scenes using high frequency patterns. The approach does not require the material properties of the objects in the scene to be known. The key idea of this method is to hide a small region of the scene from illuminated pattern while keep other parts illuminated. The intensity of the hided region is only from global illumination. When all the points in the scene hide once from illuminated light, they form a global illumination map, from here the direct illumination map is obtained by subtracting the image, in which all regions are illuminated, with the global illumination map. Even though the proposed method can reduce the number of required images, this number is still large (25 images are needed for experiments), and the patterns should have frequency high enough to sample the global components.

Seitz et al. (Seitz, 2005) proposed to use inverse light transport operator to separate m-bounced light from a scene of arbitrary BRDF. The inverse light transport operator is estimated under the assumption of Lambertian surface.

In this paper, we proposed a new method to eliminate the interreflected light components in 3D reconstruction using HOC pattern (Lee, 2005), and then the direct light component is used to reconstruct the 3D point cloud of the scene. First, the one sided edges of both direct and reflected light are estimated in every captured pattern image. Second, the bottom up approach is used to check and eliminate the interreflected boundaries from layer 3 to layer 1. Finally, the direct boundaries are used to reconstruct 3D point cloud of the scene.

The remainder of the paper is organized as follows: In Section II, we describe our proposed method to eliminate the reflected light component. The experimental results are provided in Section III. Finally, Section IV concludes the paper.

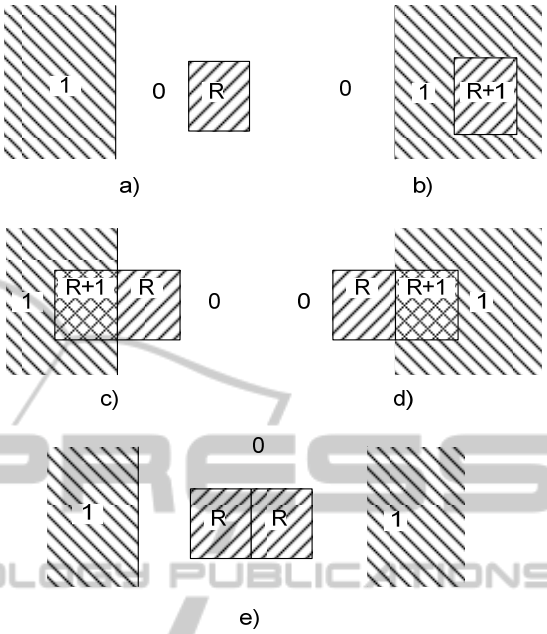

Figure 2: The appearance of interreflection together with direct light. Where "1" is direct light region, "0" is the surface region with no illuminated light, and "R" is the reflected light.

2 THE PROPOSED METHOD

2.1 The Appearance of Interreflection Together with Direct Light

When projector illuminating the pattern on the scene, depending on the surface reflectance and geometry, the interreflection might occur and appear together with illuminated pattern in different ways, as shown in Figure 2. The cases that can happen are:

- The interreflection appears on the region without illuminated pattern (Figure 2. a)
- The interreflection appears within the region of illuminated pattern (Figure 2. b)
- The interreflection appears on the boundary of the illuminated pattern (Figure 2. c-d)
- The interreflection when illuminating the pattern "1-0-1" appears edgewise on the region without illuminated pattern (Figure 2. e), where "1" means white pattern, and "0" means black pattern.

However, in reality the reflected light stripe power can be weakened and the interreflection can be unnoticeable depending the distance from

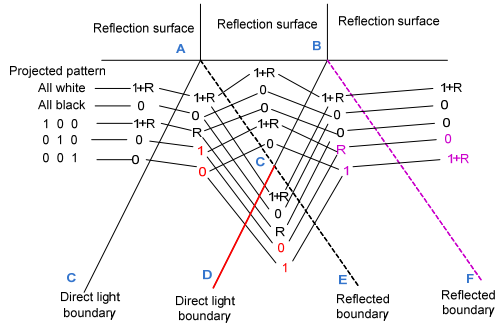

Figure 3: The model of the interreflection on the surface together with direct light component.

interreflection source (reflection surface) to the surface that interreflection appears. In this paper, we exploit in detail the particular case described in Figure 3. The reflection surface is the upper region, and the interreflection reflected from reflection surface appears on the lower region ("R") together with the illuminated pattern ("1").

When different patterns are projected, as shown in Figure 3, the boundaries can be recovered or not depending on the strength of the reflected light compared with direct light stripe, here we consider the boundaries formed by the intersection between signal "1-0" and "0-1".

- Boundary "AC": if the intensity of "R" is lower than that of "1" then "AC" can be detected by pairs "1+R-R" and "0-1" from patterns "1 0 0" and "0 1 0", otherwise "AC" cannot be detected
- Boundary "DC" is always detected by pairs "1-0" and "0-1" from patterns "0 1 0" and "0 0 1", so called direct boundary
- Boundary "AC" can be detected by pairs "R-0" and "1-1+R" from patterns "1 0 0" and "0 1 0" if the intensity of "R" is lower than that of "1"
- Boundary "CB" can be detected by pairs "1+R-R" and "0-1" from patterns "0 1 0" and "0 0 1" if the intensity of "R" is lower than that of "1"
- Boundary "CE" is always detected by pairs "R-0" and "0-R" from patterns "1 0 0" and "0 1 0", so called reflected boundary
- Boundary "BF" can be detected by pairs "R-0" and "1-1+R" from patterns "0 1 0" and "0 0 1" if the intensity of "R" is greater than that of "1"

2.2 Hierarchical Orthogonal Coded Patterns

In this paper, we use HOC (Hierarchical Orthogonal Coding) structured light patterns developed by Lee et al. (Lee, 2005), in which the orthogonal codes are arranged hierarchically in order to reduce the length of codes. The length *f* of code is divided into a few layers L. Each layer includes H orthogonal codes recursively as shown in Figure 4. Although the signal codes in the HOC are not orthogonal, each layer has a set of orthogonal codes. For more details, please refer to (Lee, 2005).

For example, we assume that a HOC has four layers (L=4) and the number of orthogonal codes in each layer is also four ($H_1 = H_2 = H_3 = H_4 = 4$). In this case, the total number of signal codes is 256 ($H_1 \times H_2 \times H_3 \times H_4 = 256$) and the code length is 16 ($H_1 + H_2 + H_3 + H_4 = 16$), i.e. we need 16 camera images for decoding addresses of the signals.

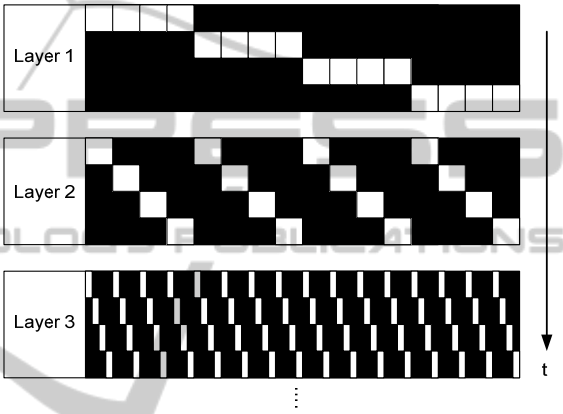

Figure 4: Hierarchical Layer of Code. Each layer consists of 4 patterns, each code in upper layer is divided in to 4 sub-codes in lower layer.

2.3 Interreflection Elimination Algorithm

2.3.1 Boundary Detection by Intersection

The most common way to obtain sub-pixel accuracy boundary position is to calculate the intersecting point between the signals of pattern "1-0" and its inverse "0-1", as shown in Figure 5.

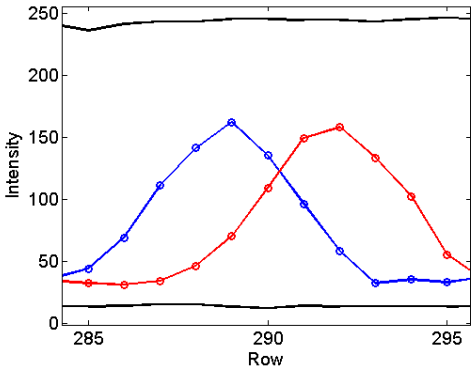

Figure 5: The boundary is detected from the intersection of pattern signal "1-0" and "0-1".

2.3.2 One Sided-edge Boundary Detection

Due to the fact that not all boundaries, including direct and reflected boundaries, can be detected by signal intersection method, moreover the direct or reflected light stripes contains all the information of the edges even they overlap each other, we can search for all possible boundaries from the edge of direct or reflected light stripes. To detect the boundary from one sided-edge, we compute the first order derivative of the edge signal, and then detect boundary by searching for the peak of the derivative, as illustrated in Figure 6. In practice, the first order at position i^{th} is computed by following equation:

$$df(i) = |f(i+d) - f(i-d)|$$

where 2**d* is step to compute derivative.

In order to avoid local peak, a window search with size of 7 pixels was used to find the peaks of the derivative.

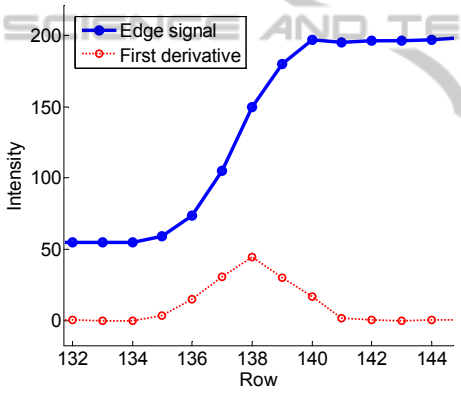

Figure 6: The signal of an edge and its first order derivative.

2.3.3 Interreflection Elimination

The HOC patterns described in Section 3 have four layers, and the width of stripes in lower layer is four times narrower than that in upper layer, thus the power of the light stripe in lower layer is four times less than that in upper layer; the light stripes in last layer patterns have weakest power, consequently the interreflection caused by this layer patterns is weakest and the interreflection distorts the direct boundaries very little. In other words, the interreflection affects on direct light component is mainly in region from AB to C in Figure 3, and this region is minimized in last layer.

Since last layer has smallest light stripes, we cannot do any further correction for this layer, thus by assuming that all boundaries in last layer patterns of HOC are correct, we can use them to eliminate interreflected boundaries and correct or fill the missing direct boundaries in upper layers using bottom up approach.

• Eliminating reflected boundary:

Once the boundary map of layer 4 (last layer) is computed by intersection, and boundary maps of other layers (from layer 1 to 3) are also computed from one-sided edges, we start to compare boundaries in pairs of layer *i* (lower layer) and layer *i-1* (upper layer), start from layer 4. If a boundary in upper layer does not match with any boundary having decoded value "0", then that boundary is classified as either reflected boundary or noise and rejected. As shown in Figure 7, boundary "a2" in upper layer does not match with "b1" or "b5" in lower layer, so it is rejected.

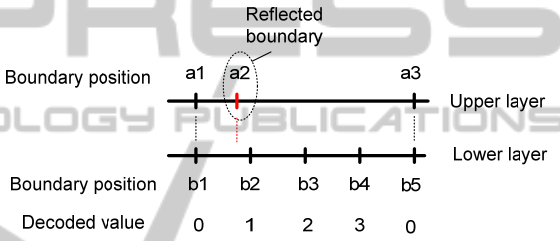

Figure 7: One direct boundary in upper layer should match with one boundary in lower layer having decoded value "0", otherwise it is either reflected boundary or noise.

• Filling the missing direct boundaries in upper layer:

Since boundary maps from layer 1 to layer 3 are detected using on-sided edges, there are chances that boundaries are not detected, these missing boundaries in one layer can be filled from the lower layer, such as filling boundaries from layer 4 to layer 3, then from layer 3 to layer 2, and finally from layer 2 to layer 1. The rule to fill boundary is described in Figure 8: search for the boundary in lower layer having decoded value "0", if there is no matched boundary in upper layer, then insert that boundary to the upper layer.

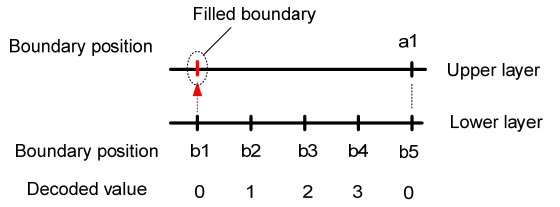

Figure 8: If one boundary in lower layer having decoded value "0" does not have any matched boundary in upper layer, fill that boundary to upper layer.

After filling the boundaries from lower layer, these new boundaries are assigned new decoded values according to theirs neighbor boundaries along the edge of light stripe. The algorithm describing the steps of removing reflected boundaries as well as recovering direct boundaries is illustrated by flowchart in Figure 9.

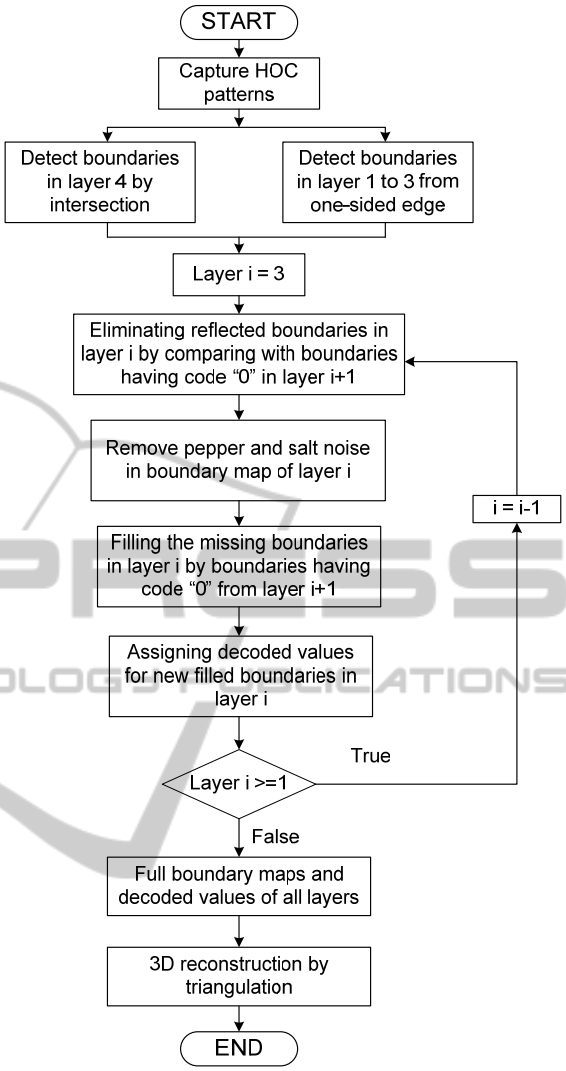

Figure 9: The flow chart of interreflection eliminating algorithm.

3 EXPERIMENTAL RESULTS

3.1 Experimental Setup

The proposed method has been implemented in a light weight structured light system which can be used for service robot applications. The system consists of an Optoma PK301 Pico projector, a PGR Flea2 1394 digital camera mounted a TV LENS 12mm 1:1.3 and a computer, as illustrated in Figure 10. The resolution of the projector was 800 x 600 pixels and that of the camera was 640 x 480 pixels. The position of the camera was about 13*cm* to the right of the projector. The computer generates signal patterns, acquires images, and computes depth images. The system has been calibrated in prior.

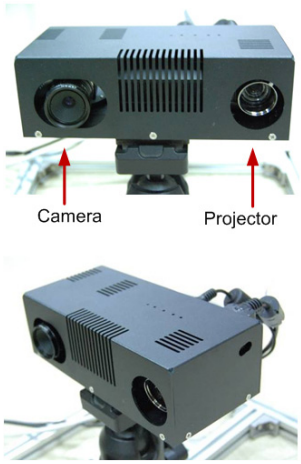

Figure 10: The setup of the structured light system.

3.2 Results

To evaluate the proposed method, we capture the images of projected HOC patterns on the scene where the interreflection occurs, an example of captured HOC pattern is shown in Figure 11.

First, the boundary map of layer 4 is computed by intersecting the stripe edge signals in pairs of consecutive patterns in that layer, as depicted in Figure 12. Since layer 4 has finest stripe patterns, there is no further information of direct boundaries to be used for correcting the interreflection effects in this layer, thus the errors caused by interreflection cannot be corrected for this layer, as shown in the horizontal band in the middle of Figure 12.

Second, the boundary maps of layers from 3 to 1 are estimated by on-sided edge in each layer, as shown in Figure 13. (a); since the boundaries are detected by searching for the edges of stripe pattern, both direct and reflected boundaries are detected. Since HOC patterns have a property that each boundary in upper layer has a common boundary in lower layer having decoded value "0", we are using this fact to remove reflected boundaries as well as noise. The reflected boundaries in layer 3 are first eliminated by comparing with the common boundaries in layer 4, the salt and pepper noise is then once more removed by a simple running

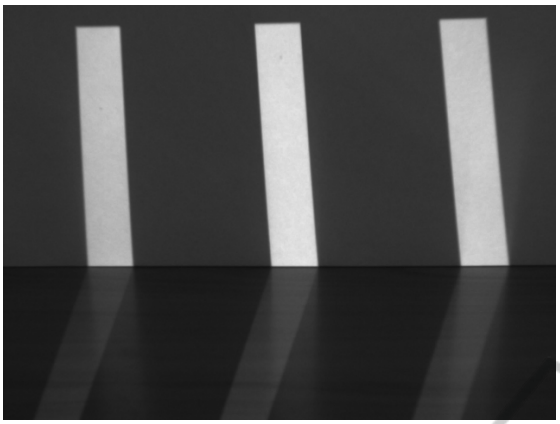

Figure 11: A captured HOC pattern in layer 2, the upper region is the source of reflection, and the interreflection appears on the lower region.

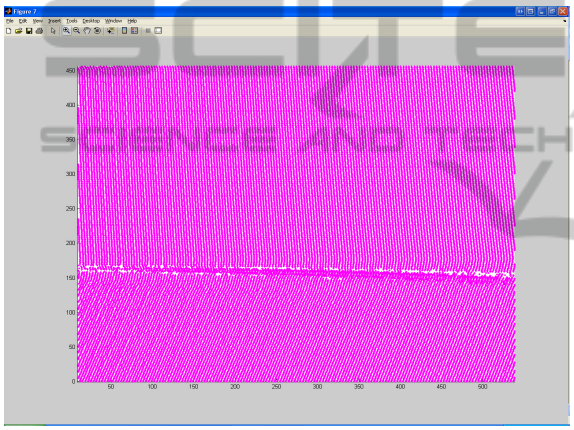

Figure 12: The boundary map of layer 4 detected by intersection.

window size 3x3. Now the boundary map of layer 3 remains only direct boundaries, but some of them are missing, as illustrated in Figure 13. (b) right. To fill the missing direct boundary in layer 3, we search for the common boundaries (having decoded value "0") in layer 4 and insert to boundary map of layer 3. Each boundary, that has been filled to layer 3, is assigned with decoded value of the neighbor boundaries along the light stripe. Repeat these processes of removing reflected boundaries and noise, and filling the missing direct boundaries for layer 2 and layer 1, we have final direct boundary maps of layer 1 to 3, as shown in Figure 13. (c).

Finally, the boundary maps of layer 1 to layer 4 together with their decoded value maps are used to decode the projector correspondence map of the scene by following the decoding algorithm of HOC (Lee, 2005), the final projector correspondence map is shown in Figure 14 (b). As can be seen, the region affected by interreflection in the result of proposed method is significantly reduced in comparison with the result of original decoding method of HOC (Figure 14 (a)). However, there is a small band in the middle of correspondence map in Figure 14 (b) where the interreflection cannot be removed, since there is no further correct information of direct boundary to correct for layer 4. Figure 15 and Figure 16 show the 3D point clouds of the scene reconstructed from the projector correspondence maps produced by proposed method and original HOC method respectively. The holes and outliers are created by effects of interreflection, they confirm the discussion above.

4 CONCLUSIONS

We have presented a new method to eliminate the interreflection effects in 3D reconstruction using structured light 3D camera endowed with HOC patterns. The proposed method first detects both direct and reflected boundaries in layer 1 to layer 3 from one-sided edges, and boundaries in layer 4 by intersection. Then the boundaries in last layer are used to eliminate the reflected boundaries in upper layers, as well as filling the missing boundaries. The experimental results have shown that the effect of interrerflection on 3D reconstruction in proposed method is greatly reduced in comparison with original decoding method of HOC. However, there is a small band region that the interreflection cannot be removed, since there is no further direct boundary information to eliminate the reflected boundary in last layer of HOC. And this drawback is the main issue for our near future work.

ACKNOWLEDGEMENTS

This research was performed for the KORUS-Tech Program (KT-2010-SW-AP-FSO-0004) funded by the Korea Ministry of Science, ICT and Planning (MSIP). This work was also supported in part by research program funded by MSIP, Korea under ITRC NIPA-2013-(H0301-13-3001), and in part by NRF-2013M1A3A02042335, the Ministry of Science ICT and Future Planning, Korea.

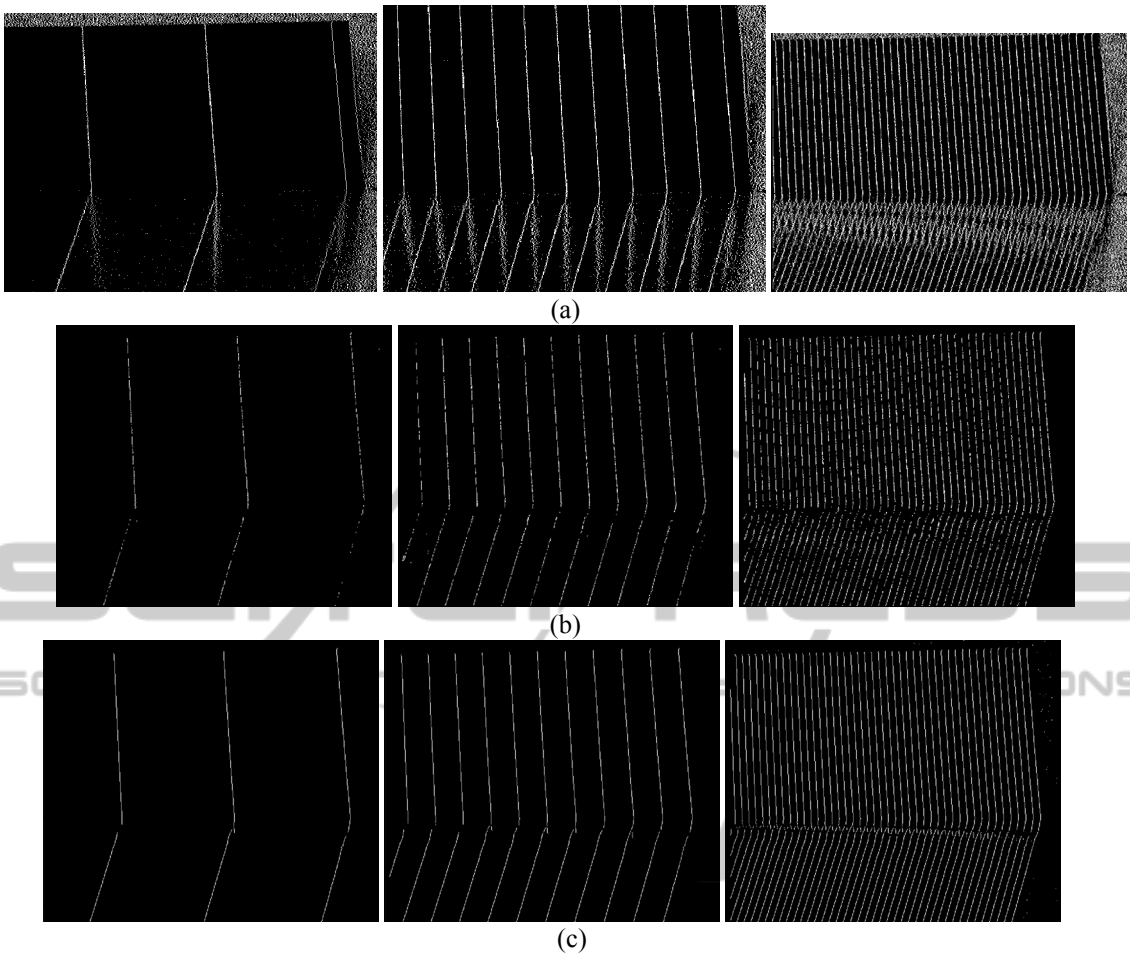

Figure 13: The boundary maps of layer 1 (left), layer 2 (middle), and layer 3 (right) detected from one-sided edge. a) The original detect boundary maps from one-sided edge. b) The boundary maps after discarding reflected boundaries and filtering the salt and pepper noise. c) The boundary maps after filling the missing boundaries from lower layer.

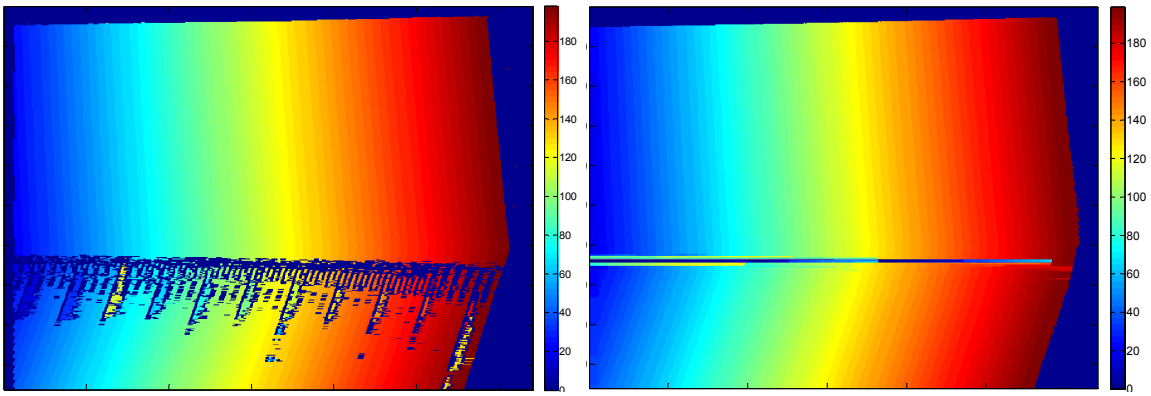

Figure 14: The projector correspondence maps of the scene decoded by original method HOC (a) and the proposed method (b).

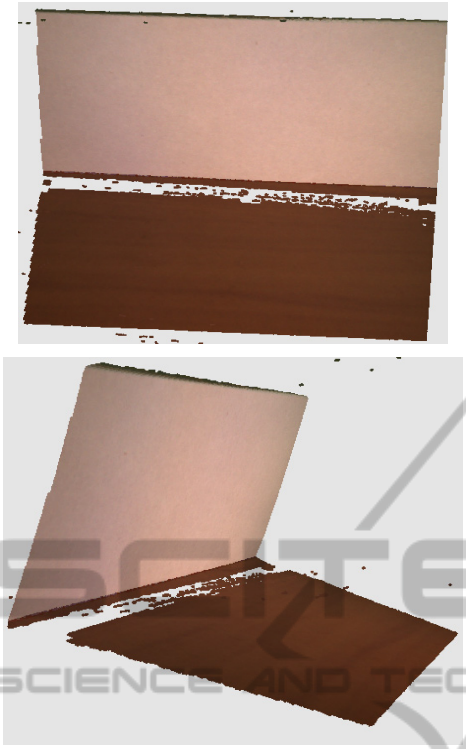

Figure 15: The 3D point cloud of the scene reconstructed by proposed method in different views.

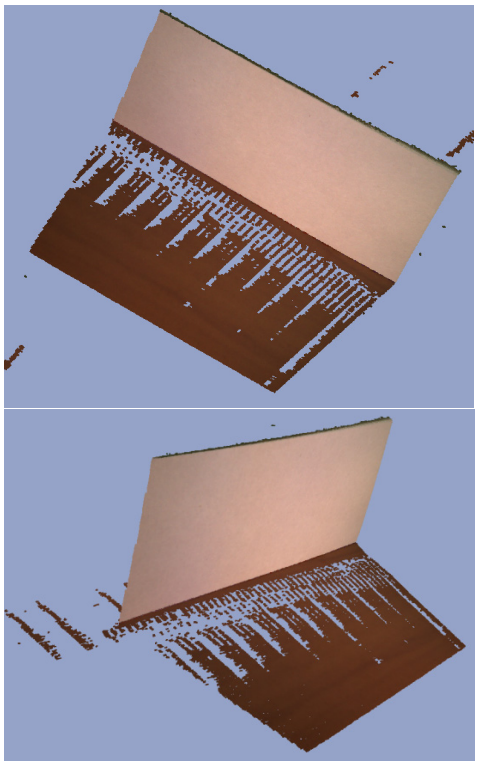

Figure 16: The 3D point cloud of the scene reconstructed by original decoding method of HOC in different views.

REFERENCES

D. Forsyth and A. Zisserman, 1989. Mutual illumination. *Computer Vision and Pattern Recognition*.

D. Forsyth and A. Zisserman, 1990. Shape from shading in the light of mutual illumination. *Image and Vision Computing*.

B. V. Funt andM. S. Drew, 1993. Color space analysis of mutual illumination. *IEEE Transactions on Pattern Analysis and Machine Intelligence*.

B. V. Funt, M. S. Drew, and J. Ho, 1991. Color constancy from mutual reflection. *International Journal of Computer Vision.*

J. Ho, B. V. Funt, and M. S. Drew, 1990. Separating a color signal into illumination and surface reflectance components: *Theory and applications. IEEE Transactions on Pattern Analysis and Machine Intelligence*.

S. Nayar, K. Ikeuchi, and T. Kanade, 1991. Shape from interreflections. *International Journal of Computer Vision*.

S. Nayar and Y. Gong, 1992. Colored interreflections and shape recovery. In *DARPA Image Understanding Workshop (IUW), pages 333–343*.

S. Nayar, G. Krishnan, M. Grossberg, and R. Raskar, 2006. Fast separation of direct and global components of a scene using high frequency illumination. In *Proceedings of ACM SIGGRAPH.*

S. Seitz, Y. Matsushita, and K. Kutulakos, 2005. A theory of inverse light transport. In *International Conference on Computer Vision*.

S. Lee, J. Choi, D. Kim et al., 2005. Signal Separation Coding for Robust Depth Imaging Based on Structured Light. *Proceedings of the IEEE International Conference on Robotics and Automation, pp. 4430-4436.*